

Combination resonances in forced vibration of spar-type floating substructure with nonlinear coupled system in heave and pitch motion

Eung-Young Choi^a, Weui-Bong Jeong^{a,*}, Jin-Rae Cho^b

^a School of Mechanical Engineering, Pusan National University, Busan, 609-735, South Korea

^b Department of Naval Architecture and Ocean Engineering, Hongik University, Sejong, 339-701, South Korea

Received 22 July 2015; revised 16 November 2015; accepted 28 January 2016

Available online 25 May 2016

Abstract

A spar-type floating substructure that is being widely used for offshore wind power generation is vulnerable to resonance in the heave direction because of its small water plane area. For this reason, the stable dynamic response of this floating structure should be ensured by accurately identifying the resonance characteristics. The purpose of this study is to analyze the characteristics of the combination resonance between the excitation frequency of a regular wave and natural frequencies of the floating substructure. First, the nonlinear equations of motion with two degrees of freedom are derived by assuming that the floating substructure is a rigid body, where the heaving motion and pitching motions are coupled. Moreover, to identify the characteristics of the combination resonance, the nonlinear term in the nonlinear equations is approximated up to the second order using the Taylor series expansion. Furthermore, the validity of the approximate model is confirmed through a comparison with the results of a numerical analysis which is made by applying the commercial software ANSYS AQWA to the full model. The result indicates that the combination resonance occurs at the frequencies of $\omega \pm \omega_{n5}$ and $2\omega_{n5}$ between the excitation frequency (ω) of a regular wave and the natural frequency of the pitching motion (ω_{n5}) of the floating substructure.

Copyright © 2016 Society of Naval Architects of Korea. Production and hosting by Elsevier B.V. This is an open access article under the CC BY-NC-ND license (<http://creativecommons.org/licenses/by-nc-nd/4.0/>).

Keywords: Spar-type floating substructures; Combination resonance; Dynamic response; Nonlinear coupled system

1. Introduction

Spar-type floating substructures are being implemented in various fields of deep water ocean engineering such as oil field development, floating-type wind-turbines, and deep-sea drilling rigs. Among the floating substructures that should maintain a stable position in a marine environment to properly perform their functions, spar-type floating structures are especially vulnerable shape-wise to the excitation of a long wave. To solve these problems so that the structure can maintain a stable position, the dynamic response characteristics of the floating substructure in the marine environment should be analyzed. These characteristics can be used to

estimate singular resonance points that can be used to design the floating substructure. A hydrodynamic numerical analysis method is frequently used to estimate such dynamic response characteristics. Jonkman (2010) wrote a technical report on the characteristics of the floating system and Browning et al. (2014) analyzed the dynamic characteristics of the floating system by using FAST software and verified through testing.

A spar-type floating substructure, whose water plane is much smaller than the submerged volume, is easier to move vertically than horizontally. This motion affects the characteristics of the restoring moment. Such a change in the restoring moment in the horizontal direction generates a time delay in the vertical motion and then a phase shift. The stability of the floating substructure's motion in this environment should be verified based on the Mathieu-type stability (Haslum and Faltinsen, 1999). Rho et al. (2002, 2003, 2004) found that a combination resonance is generated when the heave natural

* Corresponding author. Tel.: +82 51 510 3088; fax: +82 51 517 3805.

E-mail address: wbyeong@pusan.ac.kr (W.-B. Jeong).

Peer review under responsibility of Society of Naval Architects of Korea.

frequency becomes twice that of the pitch natural frequency and the excitation frequency is close to the heave natural frequency, because of the unstable coupled motions in the heave and pitch directions of the floating substructure. Hong et al. (2005) conducted a test involving regular wave excitation at different frequencies by manufacturing a floating substructure test model and verified that when the excitation frequency was close to the heave natural frequency or a value twice that of the pitch natural frequency, combination resonance occurs due to an unstable pitch motion. Moreover, through a nonlinear coupled analysis of the motions in the heave and pitch directions, Zhao et al. (2010) confirmed that when the excitation frequency is close to the sum of the heave and pitch natural frequencies, the floating substructure becomes unstable at a certain wave height or higher, thereby generating three times heave and pitch modes. Jung et al. (2013) simulated numerically models the interaction between a regular wave and the roll motion of a rectangular floating structure. Kim et al. (2014) introduced an in-house program to predict the linear and nonlinear ship motion and structural loads of a ship under the waves.

In this study, a floating substructure model is simulated to determine whether resonance is generated, not only at the frequencies that generate combination resonances, as verified in previous studies, but also at the addition and subtraction between the excitation frequencies of a regular wave and the pitch natural frequency. In addition, the causes of such combination resonances are analyzed. To analyze the motion of the floating substructure, the followings are assumed: 1) the floating substructure is a two-degree-of-freedom rigid body capable of moving in the heave and pitch directions; 2) the sum of the surface pressure of the floating substructure serves as a force and moment at the Center of Gravity (COG) and metacenter of the floating substructure; 3) the displacement, velocity, and acceleration values at the COG are reflected in

the results for all the motions of the floating substructure. Based on these assumptions, the nonlinear equations of motion for a floating substructure with a two-degree-of-freedom system are derived, and an approximate model is generated for numerically analyzing a case with a very small pitch displacement. In addition, the response in each direction is calculated through a numerical analysis utilizing MATLAB, and to analyze the characteristics of these responses, the characteristics of their frequencies are examined through the linear equations with a two-degree-of-freedom system. Finally, the result of an approximated MATLAB numerical analysis model is verified by analyzing the same model using the commercial software ANSYS AQWA Release 14.5 (2013).

2. Approximate model

In this study, the equations of motion are derived to calculate the response of the floating substructure generated by the excitation of a regular wave by assuming that the floating substructure is a two-degree-of-freedom model in the heave and pitch directions.

2.1. Equations of motion

Regarding the excitation force in a static equilibrium state, the surface pressure by a wave at the COG of the floating substructure, which is integrated in all directions, serves as the force. In terms of the amplitude, a motion in the heave direction is excited by vertical load $f_z \cos \omega t$, and a motion in the pitch direction is excited by a moment generated by $f_x \cos \omega t$. The components of the motion of the floating substructure in all directions are depicted in Fig. 1.

Where MC is the metacenter position, \overline{GM}_θ the metacentric height, G the COG in a motion, B the COB in a motion, G_0 the initial COG (center of gravity), and B_0 the initial COB (center

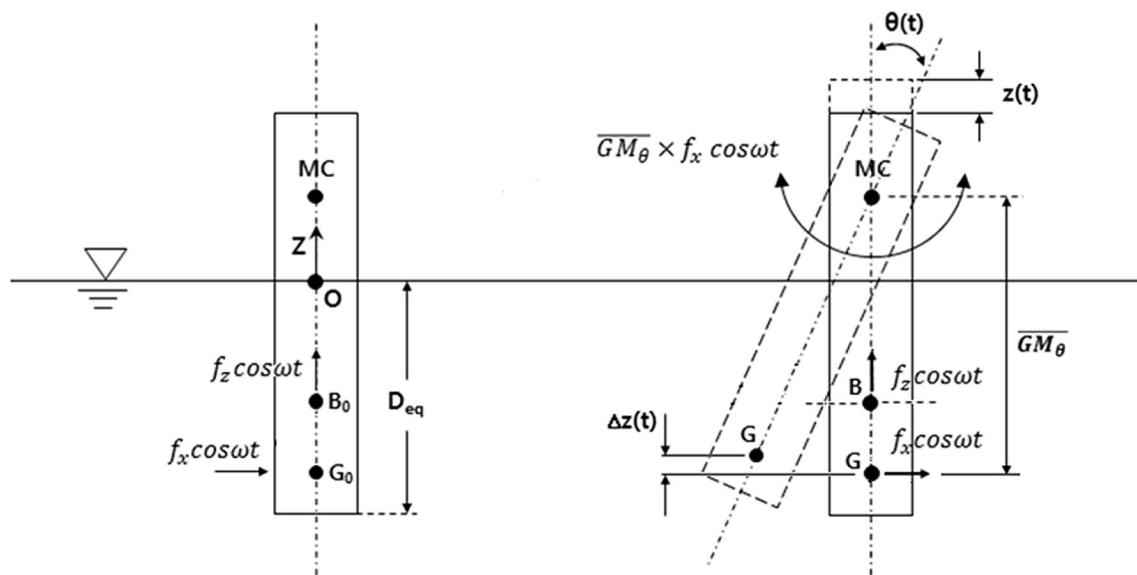


Fig. 1. Free Body Diagram of heave and pitch motion of the spar type platform.

of buoyancy), f_z is the magnitude of wave force in heave direction, f_x is the magnitude of wave force in surge direction, respectively. In addition, D_{eq} indicates the draft, $z(t)$ the heave displacement, $\theta(t)$ the pitch angle, A_w the water plane area, $\Delta z(t)$ the heave displacement under the influence of pitch angle, and ∇ the displacement volume defined by $A_w \times D_{eq}$.

Letting k and k_θ be the hydrostatic stiffness in the heave and pitch directions, the equations of motion of an undamped system in the heave and pitch directions are expressed by

$$m\ddot{z}(t) + k \cdot z(t) = f_z \cdot \cos(\omega t) \quad (1)$$

$$I\ddot{\theta}(t) + k_\theta \cdot \theta(t) = M \cdot \cos(\omega t)$$

with $M = \overline{GM}_\theta \cdot f_x$.

Moreover, k and k_θ can be represented by a function of the density of water ρ , the acceleration of gravity g , the water plane area A_w , the displacement volume ∇ and the metacentric height \overline{GM}_θ ,

$$k = \rho g A_w \quad (2)$$

$$k_\theta = \rho g \nabla \cdot \overline{GM}_\theta$$

The relationship between heave displacement $z(t)$ and heave displacement $z_G(t)$ at the COG can be derived using a geometric shape for the floating substructure, as shown in Eq. (3).

$$z(t) = z_G(t) - 2 \cdot \overline{GM}_\theta \cdot \sin^2\left(\frac{\theta(t)}{2}\right) \quad (3)$$

The length (\overline{BG}) from the COG to the center of buoyancy can be obtained and represented by a function of the length ($\overline{B_0G_0}$) and heave displacement in an equilibrium state, as shown in Eq. (4).

$$\begin{aligned} \overline{BG} &= \overline{OG} - \overline{OB} = \left(\overline{OG_0} + z(t)\right) - \frac{1}{2}(D_{eq} + z(t)) \\ &= \overline{OG_0} - \frac{1}{2}D_{eq} + \frac{1}{2}z(t) = \overline{B_0G_0} + \frac{1}{2}z(t) \end{aligned} \quad (4)$$

Furthermore, the distance (\overline{GM}_θ) from the center of rotation (MC) to the COG (G) is shown in Eq. (5), where I_w is the area moment of inertia of the floating substructure.

$$\overline{GM}_\theta = \frac{I_w}{\nabla} \left(1 + \frac{1}{2}\tan^2 \theta\right) - \overline{B_0G_0} \quad (5)$$

To simplify the equation of motion, it can be approximated by considering the second-order term of small-displacement $\theta(t)$ and applying the approximate equation shown in Eq. (6).

$$\sin^2 \theta \approx \theta^2, \quad 1 + \frac{1}{2}\tan^2 \theta \approx 1 + \frac{1}{2}\theta^2, \quad \frac{1}{1 - z(t)} \approx 1 + z(t) + z^2(t) \quad (6)$$

By applying the approximate equation to Eqs. (3)–(5), the heave displacement $z(t)$ and the metacentric height (\overline{GM}_θ) can be obtained, as shown in Eqs. (7) and (8).

$$\begin{aligned} z(t) &= z_G(t) - 2 \cdot \overline{GM}_\theta \cdot \sin^2\frac{\theta}{2} = z_G(t) - 2 \cdot \overline{GM}_\theta \cdot \frac{\theta^2}{4} \\ &= z_G(t) + \left(\overline{B_0G_0} - \frac{I_w}{A_w D_{eq}}\right) \cdot \frac{\theta^2}{2} \end{aligned} \quad (7)$$

$$\begin{aligned} \overline{GM}_\theta &= \frac{I_w}{A_w (D_{eq} - z(t))} \left(1 + \frac{\theta^2}{2}\right) - \overline{B_0G_0} \\ &= \frac{I_w}{A_w D_{eq}} \left(1 + \frac{1}{D_{eq}} z(t) + \frac{1}{D_{eq}^2} z^2(t)\right) \left(1 + \frac{\theta^2}{2}\right) - \overline{B_0G_0} \end{aligned} \quad (8)$$

By substituting the approximated equations (Eqs. (7) and (8)) into the equation of motion (Eq. (1)), it is possible to derive the approximated equations of motion of the floating substructure, which is assumed to be a rigid body with a two-degree-of-freedom system, as shown in Eqs. (9) and (10).

$$m\ddot{z}_G(t) + k \cdot z_G(t) + \left(\overline{B_0G_0} - \frac{I_w}{A_w D_{eq}}\right) \cdot k \cdot \frac{\theta^2}{2} = f_z \cdot \cos(\omega t) \quad (9)$$

$$\begin{aligned} I\ddot{\theta}(t) + D_{eq} \cdot \left(\frac{I_w}{A_w D_{eq}} - \overline{B_0G_0}\right) \cdot k \cdot \theta(t) + \overline{B_0G_0} \cdot k \cdot z_G(t) \cdot \theta(t) \\ = M \cdot \cos(\omega t) \end{aligned} \quad (10)$$

The detailed derivation of these two equations is given in Appendix, and these two coupled equations can be represented in the form of a matrix equation, as shown in Eq. (11).

$$\begin{aligned} \begin{bmatrix} m & 0 \\ 0 & I \end{bmatrix} \begin{Bmatrix} \ddot{z}_G(t) \\ \ddot{\theta}(t) \end{Bmatrix} + k \cdot \begin{bmatrix} 1 & -\beta \cdot \frac{\theta(t)}{2} \\ \overline{B_0G_0} & \beta \cdot D_{eq} \end{bmatrix} \begin{Bmatrix} z_G(t) \\ \theta(t) \end{Bmatrix} \\ = \begin{Bmatrix} f_z \cdot \cos(\omega t) \\ M \cdot \cos(\omega t) \end{Bmatrix} \end{aligned} \quad (11)$$

Eq. (11) is a nonlinear equation for the two-degree-of-freedom system, where $\beta = \left(\frac{I_w}{A_w \cdot D_{eq}} - \overline{B_0G_0}\right)$ and the overall off-diagonal elements of a stiffness matrix are represented as a function $\theta(t)$ of the pitch displacement.

2.2. Numerical analysis

The input parameters of the model selected for the numerical analysis are listed in Table 1. The model has

Table 1
Input parameters for numerical analysis.

ρ_w [kg/m ³]	1025	I [kg m ²]	5.7553×10^8
R [m]	1	$\overline{GM}_{\theta eq}$ [m]	10.3555
A_w [m ²]	3.1416	k_θ [N·m/°]	3.2448×10^7
m [kg]	3.1974×10^5	f_z [N]	1.0×10^5
ω [Hz]	0.15	M [N m]	1.0×10^7
$\overline{OG_0}$ [m]	60	D_{eq} [m]	99.2941
k_{heave} [N/m]	3.1557×10^4		

resonance frequencies in the heave and pitch directions of 0.05 [Hz] and 0.038 [Hz], respectively, based on the test data of the DeepCwind 1/50th scale model. The natural frequencies in all directions have the condition of $\theta(t) = 0$ in the equilibrium state. The parameters listed in Table 1 include the following: the density of water (ρ_w), the radius of the floating substructure (R), water plane area (A_w), mass (m), the hydrostatic stiffness in the heave direction (k_{heave}), the draft in the equilibrium state (D_{eq}), the distance from the sea surface to the COG ($\overline{OG_0}$), the excitation frequency (ω), the mass moment of inertia (I), the metacentric height in the equilibrium state ($\overline{GM_{\theta eq}}$), the hydrostatic stiffness in the pitch direction (k_θ), the amplitude of the heave excitation force (f_z), and the amplitude of the pitch excitation moment (M).

To obtain a solution of nonlinear Eq. (11) for the two-degree-of-freedom system, a numerical analysis was performed by applying the fourth-order Runge–Kutta method in MATLAB. The time responses in all directions for the numerical analysis model indicated in Table 1 are shown in Fig. 2.

To analyze the frequencies that generate combination resonance due to the coupling between the natural frequencies in all directions and the excitation frequency, the Fourier transforms of time responses are represented in Fig. 3(a), where “ \oplus ” refers to the amplitude of the heave displacement, and “ \otimes ” refers to the amplitude of each pitch displacement. The Fast Fourier Transform (FFT) results indicate that the resonance in the heave direction occurs at a natural frequency of 0.05 [Hz] ($=\omega_{n3}$), frequencies of 0.15 [Hz] ($=\omega$) and 0.3 [Hz] ($=2\times\omega$), which are the $1\times$ and $2\times$ components of the excitation frequencies, respectively, and

frequencies of 0.076 [Hz] ($=2\times\omega_{n5}$), 0.112 [Hz] ($=\omega - \omega_{n5}$), and 0.188 [Hz] ($=\omega + \omega_{n5}$). The resonance in the pitch direction occurs at a natural frequency of 0.038 [Hz] ($=\omega_{n5}$) and excitation frequency of 0.15 [Hz] ($=\omega$). The results of analyzing the frequencies at which resonance was generated other than the natural frequency and excitation frequency in all directions among the frequencies of resonance indicate that 0.076 [Hz] was double the natural pitch frequency, and 0.112 [Hz] and 0.188 [Hz] are related to the addition and subtraction between the natural pitch frequency and excitation frequency.

To determine whether the same result is produced even when the excitation frequency is adjusted, a numerical analysis was performed on the same model by adjusting the excitation frequency to 0.1 [Hz] ($=\omega$), and the analytic result is shown in Fig. 3(b). The FFT result verifies that resonance is generated in the heave direction at a natural frequency of 0.05 [Hz] ($=\omega_{n3}$), frequencies of 0.1 [Hz] ($=\omega$) and 0.2 [Hz] ($=2\times\omega$), which are the $1\times$ and $2\times$ components of the excitation frequencies, respectively, and frequencies of 0.062 [Hz] ($=\omega - \omega_{n5}$), 0.076 [Hz] ($=2\times\omega_{n5}$), and 0.138 [Hz] ($=\omega + \omega_{n5}$). Resonances are generated in the pitch direction at the natural frequency of 0.038 [Hz] ($=\omega_{n5}$) and excitation frequency of 0.1 [Hz] ($=\omega$).

The results of analyzing the frequencies at which resonance is generated other than the natural frequency and excitation frequency in all directions among the frequencies of resonance indicate that 0.076 [Hz] is double the natural pitch frequency, and 0.062 [Hz] and 0.138 [Hz] are related to the addition and subtraction between the natural pitch frequency and excitation frequency.

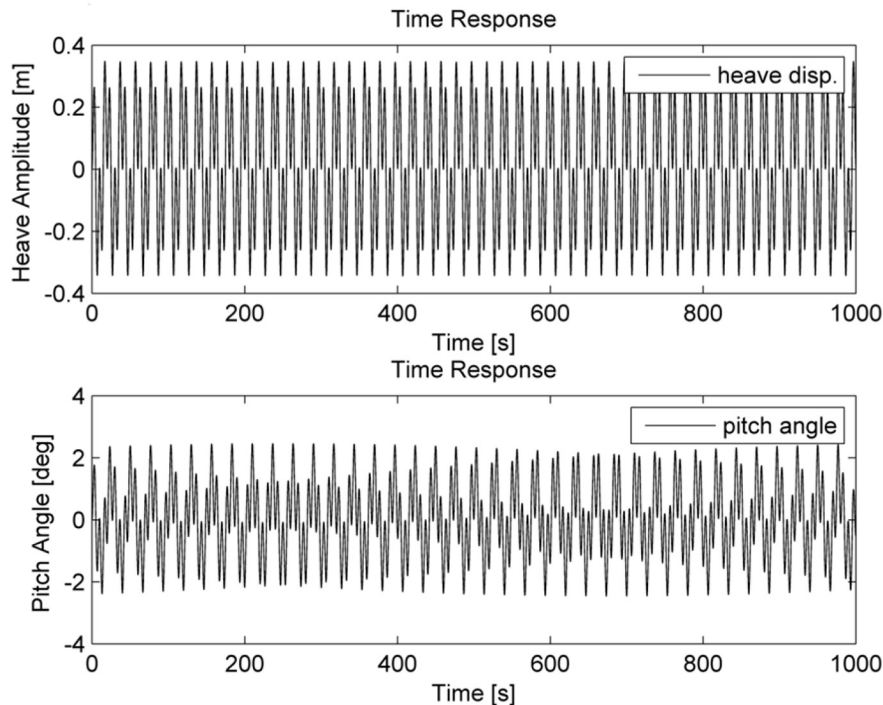


Fig. 2. Numerical results of time response of heave and pitch motion.

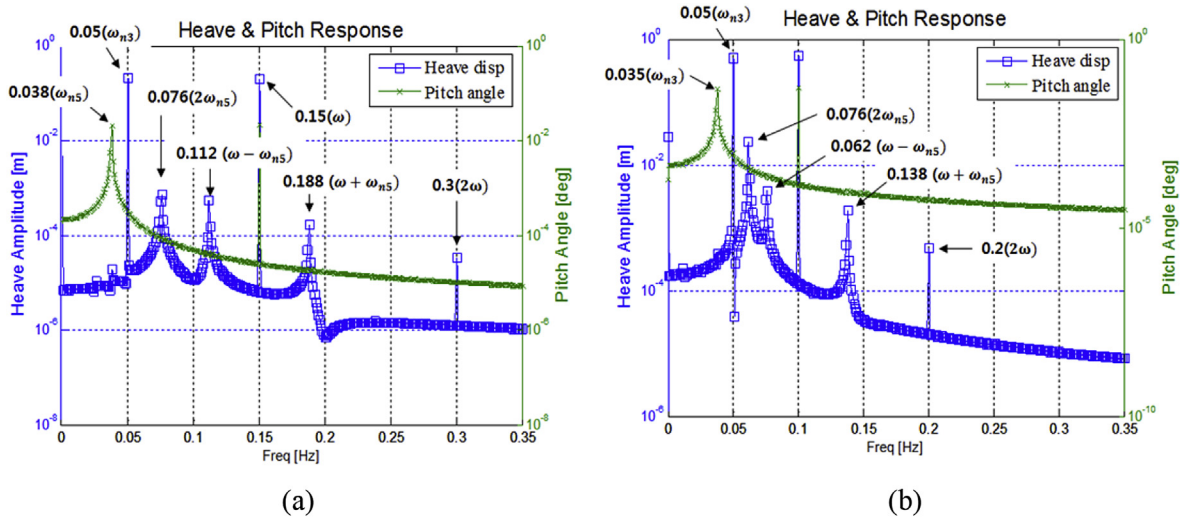


Fig. 3. Fourier Transform of time response of heave and pitch motion: (a) Wave frequency: 0.15 [Hz] (b) Wave frequency: 0.1 [Hz].

3. Characteristics of the combination resonance

The fact that resonance is also generated at the frequency of addition and subtraction between the excitation frequency and the pitch natural frequency, and a frequency that is double the pitch natural frequency, in addition to the natural frequency and excitation frequency, due to the geometric shape of the floating substructure, is verified by the analysis results for two numerical analysis models with different excitation frequencies.

In this section, the floating substructure is assumed to be an undamped linear system of small-vibration with a two-degree-of-freedom system to analyze the frequencies that can lead to combination resonance. The frequencies that generate combination resonance are identified by performing a frequency analysis of the solution obtained using this model.

3.1. Two-degree-of-freedom approximate model

Eqs. (12) and (13) are the equations of motion for the forced vibration of the undamped system, where the natural frequencies in the heave and pitch directions in the static equilibrium state are ω_{n3} and ω_{n5} , respectively; the normal force in the heave direction is $F_0 \cdot \cos \omega t$; and the moment in the pitch direction is $M_0 \cdot \cos \omega t$.

$$\ddot{z}(t) + \omega_{n3}^2 z(t) = F \cdot \cos(\omega t) \quad (12)$$

$$\ddot{\theta}(t) + \omega_{n5}^2 \theta(t) = M \cdot \cos(\omega t) \quad (13)$$

Where $F = F_0/m$ and $M = M_0/I$ represent the normalized force and moment respectively, while m is mass and I is the mass moment of inertia.

If the equations of motion for all directions have the initial conditions of $z(0) = \theta(0) = 0$ and $\dot{z}(0) = \dot{\theta}(0) = 0$, a general solution for the responses in all directions can be represented as shown in Eqs. (14) and (15).

$$z(t) = A \cos(\omega t) - A \cos(\omega_{n3} t) \quad (14)$$

$$\theta(t) = B \cos(\omega t) - B \cos(\omega_{n5} t) \quad (15)$$

Where

$$A = \frac{F}{\omega_{n3}^2 - \omega^2}, \quad B = \frac{M}{\omega_{n5}^2 - \omega^2}$$

Moreover, the displacement $\Delta z(t)$ in the heave direction, which is generated by the rotational displacement $\theta(t)$ in the pitch direction due to the geometric shape of the floating substructure, can be represented by a function of the distance (L) from the metacenter (MC) to the COG and the pitch displacement $\theta(t)$, as shown in Eq. (16).

$$\Delta z(t) = 2 \times L \times \sin \frac{\theta(t)}{2} \times \sin \frac{\theta(t)}{2} \quad (16)$$

The displacement ($z_G(t)$) in the heave direction from the COG is calculated based on the difference between the displacement $z(t)$ in the heave direction and the displacement $\Delta z(t)$ in the heave direction generated by $\theta(t)$, as shown in Eq. (17).

$$z_G(t) = z(t) - \Delta z(t) \quad (17)$$

The displacement in the heave direction from the COG of the floating substructure can be obtained by substituting Eqs. (13) and (14) into Eq. (16), as shown in Eq. (18).

$$z_G(t) = A \cos(\omega t) - A \cos(\omega_{n3} t) - 2 \cdot L \cdot \left[\sin \left(\frac{B \cos(\omega t) - B \cos(\omega_{n5} t)}{2} \right) \right]^2 \quad (18)$$

Where L is the metacentric height, ω the wave frequency, ω_{n3} and ω_{n5} the heave and pitch resonance frequencies in static equilibrium.

In addition, Eq. (19) shows a generalized Taylor series expansion, where $f = \sin^2 \theta$ in relation to small-displacement θ .

$$f = \sum_{n=1}^{\infty} (-4)^{n-1} \cdot \frac{f^{(2)}(0)}{2n!} \cdot \theta^{2n} \quad (19)$$

By applying Eqs. (18) and (19), the displacement $z_G(t)$ in the heave direction at the COG for small-displacement θ can be generalized as shown in Eq. (20).

$$z_G(t) = A \cos(\omega t) - A \cos(\omega_{n3} t) - 2 \cdot L \cdot \left[\sum_{n=1}^{\infty} (-4)^{n-1} \cdot \frac{1}{n!} \cdot \theta^{2n} \right] \quad (20)$$

Where

$$\theta = \frac{B \cos(\omega t) - B \cos(\omega_{n5} t)}{2}$$

An approximate solution considering the second-order term ($n = 1$) can be derived by using the Taylor series expansion in linear Eq. (18), as shown in Eq. (21), and represented by the addition and subtraction of cosine functions, as shown in Eq. (22).

$$z_G(t) = A \cos(\omega t) - A \cos(\omega_{n3} t) - 2L \left[\left(\frac{B \cos(\omega t) - B \cos(\omega_{n5} t)}{2} \right)^2 \right] \quad (21)$$

$$z_G(t) = A \cos \omega t - A \cos \omega_{n3} t - \frac{B^2 L}{4} \cos(2\omega) t + \frac{B^2 L}{2} \cos(\omega \pm \omega_{n5}) t - \frac{B^2 L}{4} \cos(2\omega_{n5}) t - \frac{B^2 L}{2} \quad (22)$$

The result of Eq. (22) indicates that displacement $z_G(t)$ in the heave direction from the COG consists of a combination of cosine functions with frequencies of ω , ω_{n3} , 2ω , $2\omega_{n5}$, and $\omega \pm \omega_{n5}$. This means that combination resonance can occur at the frequencies of $2\omega_{n5}$ and $\omega \pm \omega_{n5}$, in addition to the excitation frequency ω and heave natural frequency ω_{n3} , which shows the same pattern for the frequency characteristics as that shown in the results of the nonlinear numerical analysis in Section 2.

3.2. Error analysis of the approximate solution by approximate model

In Section 3.1, the frequencies that lead to combination resonance were identified based on the Taylor series expansion up to the second-order term ($n = 1$). This section identifies the frequencies that generate combination resonance when high-order terms in the Taylor series expansion are included or the error in the approximate solution is reduced. In addition, by comparing the approximate solution and a correct solution through a numerical analysis, the error due to the application of the approximate solution is analyzed. To reduce the error from the application of the Taylor expansion approximate solution, an approximate equation that includes the terms up to the fourth order ($n = 2$) is obtained, as shown in Eq. (23).

$$z_G(t) = A \cos(\omega t) - A \cos(\omega_{n3} t) - 2L \left[\left(\frac{B \cos(\omega t) - B \cos(\omega_{n5} t)}{2} \right)^2 - \frac{1}{3} \left(\frac{B \cos(\omega t) - B \cos(\omega_{n5} t)}{2} \right)^4 \right] \quad (23)$$

When Eq. (23) is split by the addition and subtraction of the cosine function, it is as shown in Eq. (24).

$$z_G(t) = A \cos(\omega t) - A \cos(\omega_{n3} t) + \frac{B^4 L}{192} \cos(4\omega t) + \frac{B^4 L}{192} \cos(4\omega_{n5} t) + \frac{B^2 L(B^2 - 3)}{12} \cos(2\omega t) + \frac{B^2 L(B^2 - 3)}{12} \cos(2\omega_{n5} t) - \frac{B^4 L}{48} \cos(\omega \pm 3\omega_{n5}) t - \frac{B^4 L}{48} \cos(3\omega \pm \omega_{n5}) t + \frac{B^4 L}{32} \cos(2\omega \pm 2\omega_{n5}) t - \frac{B^2 L(B^2 - 4)}{8} \cos(\omega \pm \omega_{n5}) t + \frac{3B^2 L(B^2 - 8)}{32} \quad (24)$$

Eq. (24) confirms that when an approximate solution that includes the high-order terms ($n = 2$) is applied, the combination resonance is also generated by frequencies $2(\omega \pm \omega_{n5})$, $\omega \pm 3\omega_{n5}$, 4ω , $4\omega_{n5}$, and $3\omega \pm \omega_{n5}$ in addition to the frequencies that lead to combination resonance using an approximate solution with the terms up to the second order ($n = 1$).

To analyze the effects of the Taylor expansion error, the correct solution of a simple numerical analysis model, the approximate solution including the terms up to the second order, and the approximate solution including the terms up to the fourth order are compared. The input parameters applied for the numerical analysis model are listed in Table 2.

Fig. 4 shows the time responses in the pitch direction when the parameters listed in Table 2 are applied.

Fig. 5 indicates that when $\theta(t)$ is very small, as shown in Fig. 4, the same numerical analysis results are obtained regardless of the approximation. However, as shown in Fig. 7, when $\theta(t)$ becomes greater by applying the parameters of Table 3, only the peaks of $\omega \pm \omega_{n5}$ [Hz] are found as a result of the removal of the high-order terms in the approximate equation using the terms up to the second order compared to the exact solution, but the other peaks are absent at the other frequencies. It seems that this result is obtained because the error of the approximate solution is affected by an increase in $\theta(t)$.

The input parameters when $\theta(t)$ does not have a small value are listed in Table 3, and the time responses in the pitch direction are shown in Fig. 6.

To decrease the error of the approximate solution, the result of Eq. (23), which was approximated by developing the Taylor

Table 2
Input parameters for numerical analysis with small $\theta(t)$.

ω [rad/s]	ω_{n3} [rad/s]	ω_{n5} [rad/s]	F [N/kg]	M [N/kg m]	L [m]
$0.5 \times 2\pi$	$0.03 \times 2\pi$	$0.04 \times 2\pi$	1.0	0.001	10

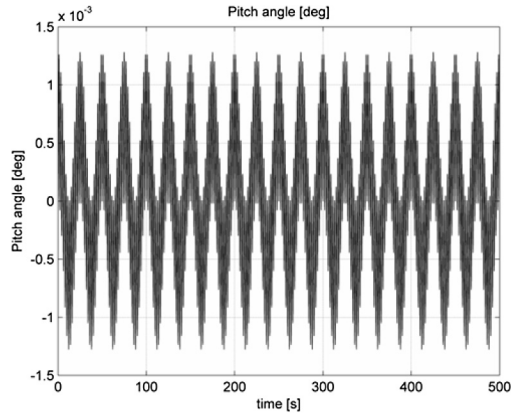


Fig. 4. Numerical response of pitch motion in the case of Table 2.

series expansion up to the fourth order term ($n = 2$), was compared with the exact solution. As a result, it is found that when the fourth order term ($n = 2$) is included, resonance is generated at a frequency similar to that of the exact solution as a result of a decrease in the error, as shown in Fig. 7.

Thus, the fact that combination resonance can occur not only at the natural frequency and excitation frequency, but also at the frequencies of $2(\omega \pm \omega_{n5})$, $\omega \pm 3\omega_{n5}$, 4ω , $4\omega_{n5}$, and $3\omega \pm \omega_{n5}$, as a result of the geometric shape of the floating substructure during excitation by a regular wave with a singular frequency, is verified using a linear model as an example.

4. Verification of numerical analysis results

To verify the results of a numerical analysis using MATLAB, the same model was analyzed by utilizing the commercial software ANSYS AQWA Ver. 14.5.

4.1. Analytic model and procedure of AQWA

The input parameters for the ANSYS AQWA simulation are described in Fig. 8.

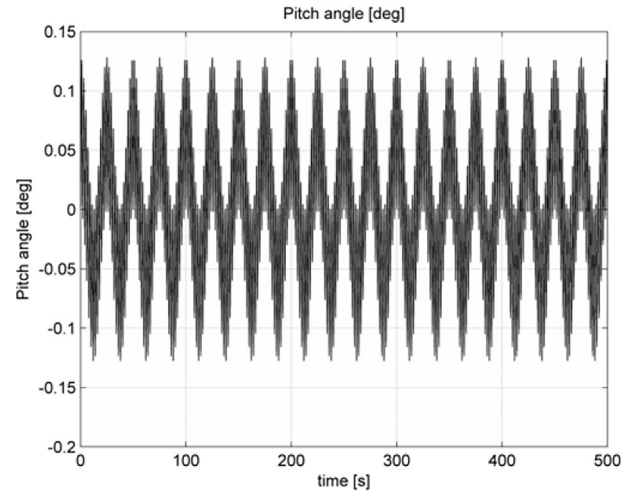


Fig. 6. Numerical response of pitch motion in the case of Table 3.

The response amplitude operator (RAO) of a structure in waves is calculated by solving the equation of motion (Eq. (25)) in the frequency domain.

$$[-\omega^2(M_s + M_a(\omega)) - i\omega C(\omega) + K] \cdot X(\omega) = F(\omega) \quad (25)$$

Where M_s is the mass of structure, M_a the frequency-dependent added mass, C the frequency-dependent damping, K the hydrostatic stiffness, and F the hydrodynamic force (incident and diffracting forces).

The calculated RAO can then be used to calculate the frequency response of the total hydrodynamic force, which consists of the hydrodynamic force f , the inertial force by added mass, and the damping force generated based on the Airy wave theory. The total hydrodynamic force is shown in Eq. (26).

$$F(t) = Re[f - M_a \ddot{X} - C \dot{X}] \cdot e^{(-\omega t + kx)} \quad (26)$$

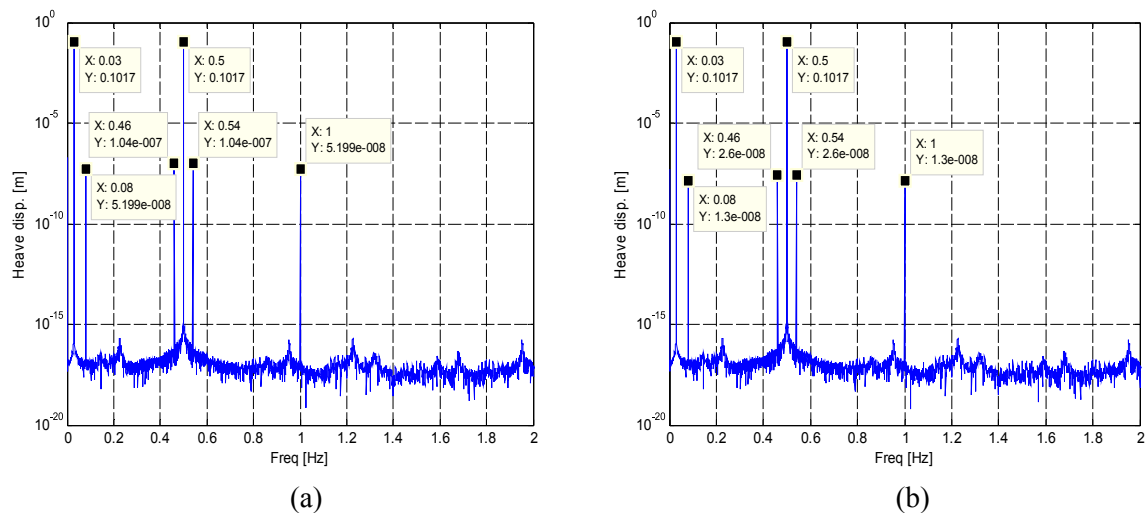


Fig. 5. Accuracy of approximate model with 2nd order Taylor expansion for a small vibration: (a) Approximate solution (b) Exact solution.

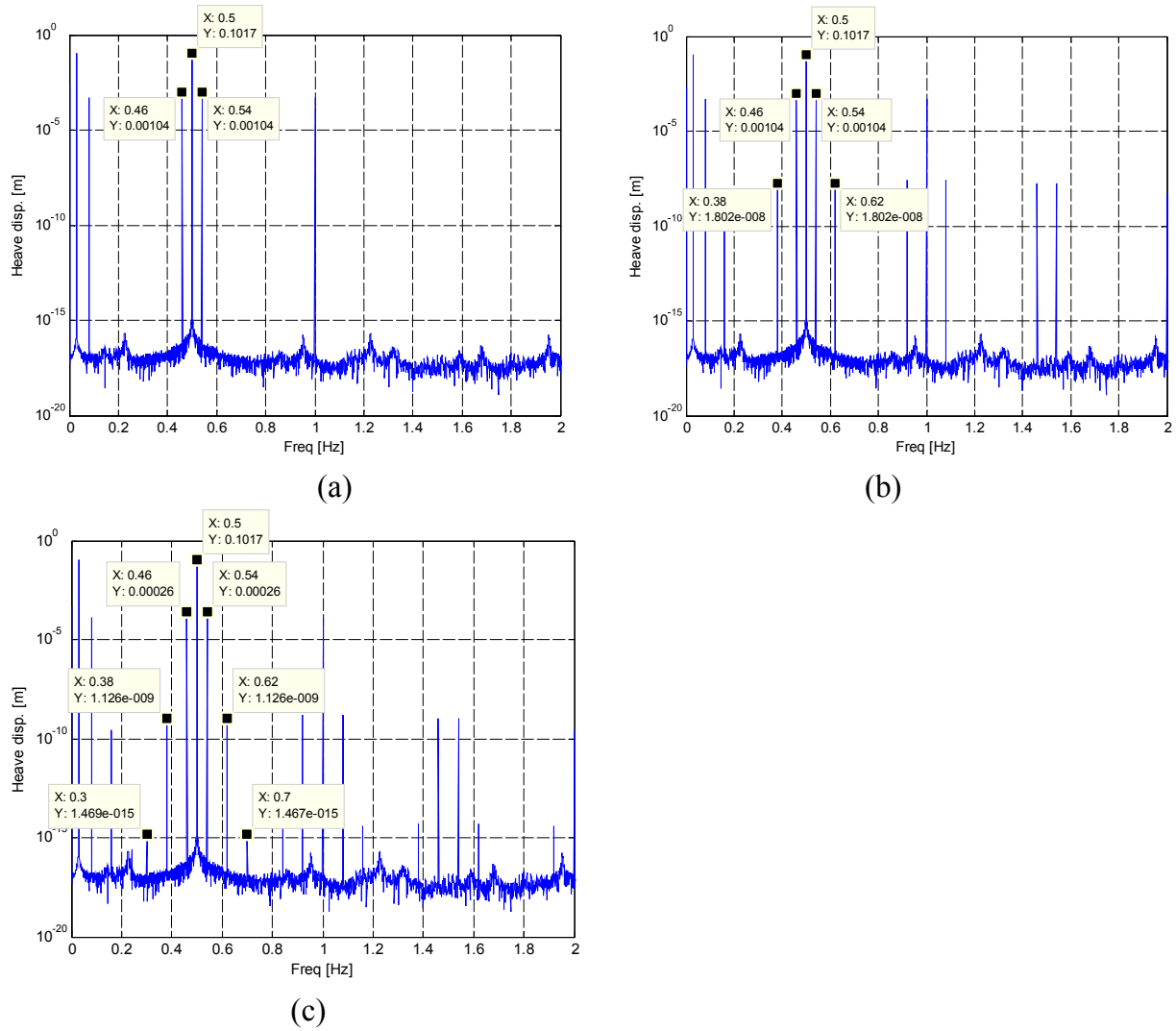


Fig. 7. Accuracy of approximate model with 4th order Taylor expansion for a large vibration: (a) Approximate solution (2nd order) (b) Approximate solution (4th order) (c) Exact solution.

Where \dot{X} is the complex velocity ($=i\omega X$), \ddot{X} the complex acceleration ($= -\omega^2 X$), k the wave number and C the system linear damping matrix, respectively.

4.2. Comparison of AQWA analysis results

The AQWA analysis using a full analysis model and the numerical analysis using the approximate model by MATLAB are compared in Fig. 9.

In Fig. 9, “ \ominus ” and “ \times ” are the displacement amplitude in the heave direction and the amplitude of pitch angular displacement calculated by MATLAB, respectively, while “ \oplus ” and “ $+$ ” are the displacement amplitude in the heave

direction and amplitude of pitch angular displacement calculated by AQWA, respectively. Compared to the result of the approximate model, the AQWA result shows a very small difference in the natural frequency in the pitch direction (approximate model: 0.038 [Hz] ($=\omega_{n5}$), AQWA: 0.032 [Hz] ($=\omega_{n5}$)). Resonance in the heave direction is generated at the natural frequency of 0.05 [Hz] and the $1\times$ and $2\times$ components of excitation frequency of 0.15 [Hz] ($=\omega$) and 0.3 [Hz] ($=2\omega$) and frequencies of 0.064 [Hz], 0.118 [Hz], and 0.182 [Hz]. Resonance in the pitch direction is generated at the natural frequency of 0.032 [Hz] and excitation frequency of 0.15 [Hz]. By analyzing the frequency at which resonance is generated other than the natural frequency and excitation frequency in all directions among the resonance frequencies, it was confirmed that 0.064 [Hz] ($=2\omega_{n5}$) is double the natural pitch frequency, and 0.118 [Hz] ($=\omega - \omega_{n5}$) and 0.188 [Hz] ($=\omega + \omega_{n5}$) are related to the addition and subtraction between the pitch natural frequency and the excitation frequency.

Table 3
Input parameters for numerical analysis with large $\theta(t)$.

ω [rad/s]	ω_{n3} [rad/s]	ω_{n5} [rad/s]	F [N]	M [Nm]	L [m]
$0.5 \times 2\pi$	$0.03 \times 2\pi$	$0.04 \times 2\pi$	1.0	0.1	10

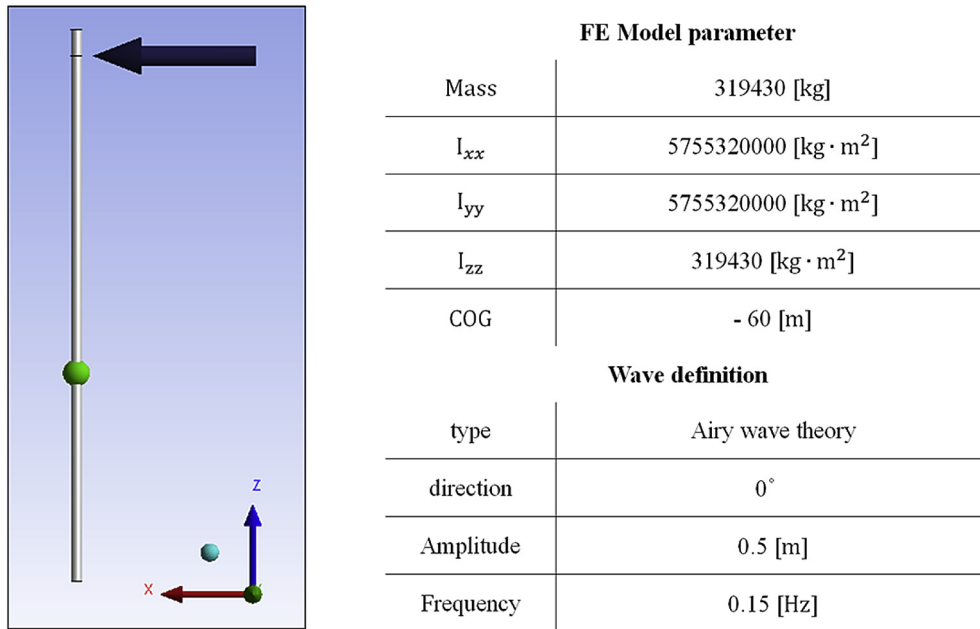


Fig. 8. ANSYS AQWA FE Modeling parameter.

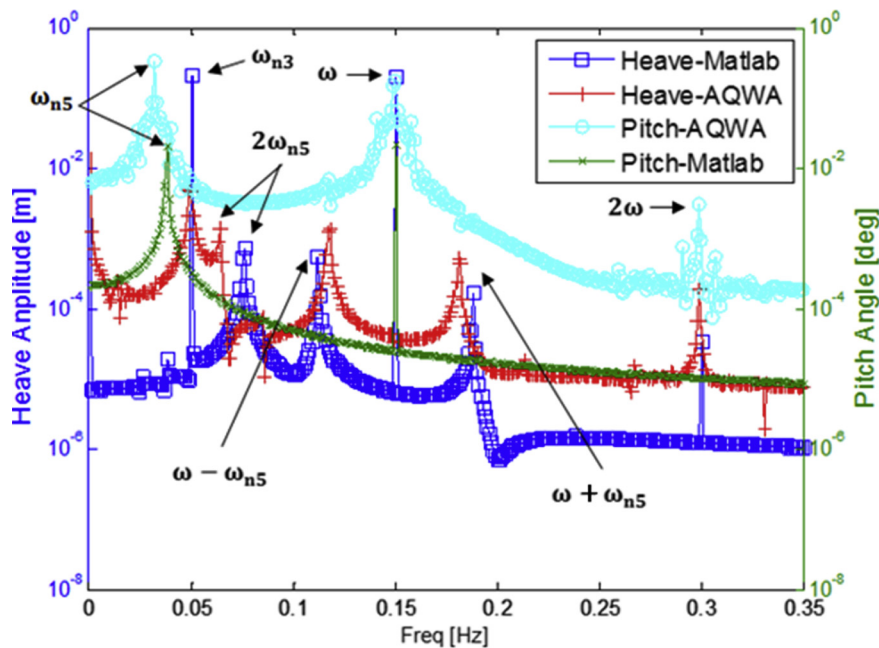


Fig. 9. Comparison of results by AQWA and MATLAB.

5. Conclusion

- (1) For a spar-type floating substructure where forced vibration occurs due to a regular wave, the equations of motion of a two-degree-of-freedom approximate model considering the coupling of the heave and pitch motions were derived, and the characteristics of the frequency response were analyzed.
- (2) It was confirmed that combination resonance occurs not only at the excitation frequency (ω) of a regular wave and the natural frequency of (ω_{n5}) in the pitch direction of the

- floating substructure, but also at the frequency of ($\omega \pm \omega_{n5}$), which is the addition and subtraction between these two frequencies, and at the frequencies of ($2\omega_{n5}$) and ($2\omega \pm 2\omega_{n5}$), which are double the pitch natural frequency and the addition and subtraction between two frequencies.
- (3) The analytic results using the nonlinear equations of motion with terms approximated from the second to fourth order using Taylor series expansion were compared with the analytic results of the full model using ANSYS AQWA in order to identify the characteristics of the combination resonance. The comparison verified that the approximate

model using the terms up to the second order can sufficiently identify the combination resonance characteristics of the full model.

- (4) It was confirmed that combination resonance occurs because a pitching motion affects the heaving motion due to the geometric correlation of the floating substructure.

Acknowledgment

This work was supported by the Human Resources Development program (No. 20134030200290) of the Korea Institute of Energy Technology Evaluation and Planning (KETEP) grant funded by the Korea government Ministry of Trade, Industry and Energy.

Appendix. Derivation of Eq. (10)

The hydrostatic stiffness k_θ in the pitch direction at the pitch angle $\theta(t)$ becomes

$$k_\theta = \rho g \nabla \cdot \overline{GM}_\theta = \rho g A_w (D_{eq} - z(t)) \cdot \overline{GM}_\theta \quad (A1)$$

and substituting the metacentric height (\overline{GM}_θ) defined in Eq. (8) gives us

$$k_\theta = \rho g A_w (D_{eq} - z(t)) \cdot \frac{I_w}{A_w D_{eq}} \left(1 + \frac{z(t)}{D_{eq}} + \frac{z^2(t)}{D_{eq}^2} \right) \cdot \left(1 + \frac{\theta^2}{2} \right) - \rho g A_w (D_{eq} - z(t)) \cdot \overline{B_0 G_0} \quad (A2)$$

By neglecting the high order terms, together with the relation of $k = \rho g A_w$, one can get

$$k_\theta = k D_{eq} \cdot \frac{I_w}{A_w D_{eq}} \cdot \left(1 + \frac{z(t)}{D_{eq}} \right) - k z(t) \cdot \frac{I_w}{A_w D_{eq}} - k (D_{eq} - z(t)) \cdot \overline{B_0 G_0} \quad (A3)$$

Substituting $z(t)$ in Eq. (7) and neglecting the term $\frac{\theta^2}{2}$ leads to

$$k_\theta = D_{eq} \frac{I_w}{A_w D_{eq}} \cdot \left(1 + \frac{Z_G(t)}{D_{eq}} \right) \cdot k - \frac{I_w}{A_w D_{eq}} \cdot k \cdot z_G(t) - (D_{eq} - z_G(t)) \cdot \overline{B_0 G_0} \cdot k \quad (A4)$$

By rearranging the terms, one can get

$$k_\theta = D_{eq} \cdot \left(\frac{I_w}{A_w D_{eq}} - \overline{B_0 G_0} \right) \cdot k + \overline{B_0 G_0} \cdot k \cdot z_G(t) \quad (A5)$$

Note that the second term in the first parenthesis and the second term were cancelled out each other in the procedure of rearrangement.

Finally, substituting Eq. (A5) into the equation of pitch motion in Eq. (1) provides us

$$\begin{aligned} I \ddot{\theta}(t) + D_{eq} \cdot \left(\frac{I_w}{A_w D_{eq}} - \overline{B_0 G_0} \right) \cdot k \cdot \theta(t) + \overline{B_0 G_0} \cdot k \cdot z_G(t) \cdot \theta(t) \\ = M \cdot \cos(\omega t) \end{aligned} \quad (A6)$$

References

- ANSYS, Inc. Release 14.5 ANSYS AQWA User's Manual.
- Browning, J.R., Jonkman, J., Robertson, A., Goupee, A.J., 2014. Calibration and validation of a spar-type floating offshore wind turbine model using the FAST dynamic simulation tool. *J. Phys. Conf. Ser.* 555.
- Haslum, H.A., Faltinsen, O.M., 1999. Alternative shape of spar platforms for use in hostile areas. In: *Proceedings of the 31st Offshore Technology Conference*, Houston, TX, May 3–6, Vol. 2.
- Hong, Y.P., Lee, D.Y., Choi, Y.H., 2005. An experimental study on the extreme motion responses of a SPAR platform in the heave resonant waves. In: *Proceedings of the 15th International Offshore and Polar Engineering Conference*, Seoul, Korea, June 19–24, pp. 225–232.
- Jonkman, J., 2010. Definition of the Floating System for Phase IV of OC3. Technical Report, NREL/TP-500-47535.
- Jung, Jae-Hwan, Yoon, Hyun-Sik, Chun, Ho-Hwan, Lee, Inwon, Park, Hyun, 2013. Numerical simulation of wave interacting with a free floating body. *Int. J. Nav. Archit. Ocean Eng.* 5, 333–347.
- Kim, Y., Kim, K.H., Kim, J.H., Kim, T., Seo, M.G., Kim, Y., 2014. Time-domain analysis of nonlinear motion responses and structural loads on ships and offshore structures: development of WISH programs. *Int. J. Nav. Archit. Ocean Eng.* 3 (1), 37–52.
- Rho, J.B., Choi, H.S., Lee, W.C., 2002. Heave and pitch motion of a spar platform with damping plate. In: *Proceedings of the 12th International Offshore and Polar Engineering Conference*, Kitakyushu, Japan, May 26–31, Vol. 12, pp. 198–201.
- Rho, J.B., Choi, H.S., Lee, W.C., 2003. An experimental study for mooring effects on the stability of spar platform. In: *Proceedings of the 13th International Offshore and Polar Engineering Conference*, Honolulu, HI, May 25–30, pp. 285–288.
- Rho, J.B., Choi, H.S., Lee, W.C., 2004. Vertical motion characteristics of truss spars in waves. In: *Proceedings of the 14th International Offshore and Polar Engineering Conference*, Toulon, France, May 23–28, pp. 662–665.
- Zhao, J., Tang, Y., Shen, W., 2010. A study on the combination resonance response of a classic spar platform. *J. Vib. Control* 16, 2083–2107.